Sphingomyelin homeostasis is required to form functional enzymatic domains at the trans-Golgi network

Josse van Galen,[1,2] Felix Campelo,[1,2] Emma Martínez-Alonso,[3,4] Margherita Scarpa,[1,2] José Ángel Martínez-Menárguez,[3,4] and Vivek Malhotra[1,2,5]

[1]Cell and Developmental Biology Programme, Centre for Genomic Regulation, 08003 Barcelona, Spain
[2]Universitat Pompeu Fabra, 08002 Barcelona, Spain
[3]Department of Cell Biology and Histology, Faculty of Medicine, and [4]Institute of Murciano Biosanitary Research, University of Murcia, 30100 Murcia, Spain
[5]Institució Catalana de Recerca i Estudis Avançats, 08010 Barcelona, Spain

Do lipids such as sphingomyelin (SM) that are known to assemble into specific membrane domains play a role in the organization and function of transmembrane proteins? In this paper, we show that disruption of SM homeostasis at the trans-Golgi network (TGN) by treatment of HeLa cells with D-ceramide-C6, which was converted together with phosphatidylcholine to short-chain SM and diacylglycerol by SM synthase, led to the segregation of Golgi-resident proteins from each other. We found that TGN46, which cycles between the TGN and the plasma membrane, was not sialylated by a sialyltransferase at the TGN and that this enzyme and its substrate TGN46 could not physically interact with each other. Our results suggest that SM organizes transmembrane proteins into functional enzymatic domains at the TGN.

Introduction

Newly synthesized proteins are core glycosylated in the ER after which the sugar chains are trimmed and modified at the Golgi complex. This process takes place in a spatially and timely regulated manner, as trimming of the core glycosylations by mannosidases in the cis- and medial-Golgi cisternae is a requirement for complex glycosylation in later Golgi compartments (Stanley, 2011). What is the role of membrane organization in the coordination of the glycosylation process at the Golgi membranes? We previously reported that treatment of cells with short-chain ceramide causes a replacement of endogenous sphingomyelin (SM) with short-chain SM (C6-SM) at the Golgi complex (Duran et al., 2012). Short-chain SM does not possess the ability to form liquid-ordered domains, and thus, the lateral organization of the Golgi membranes is disrupted (Duran et al., 2012). Disruption of the lipid order by short-chain ceramide treatment blocks Golgi membrane fission and generation of transport carriers but not the fusion of incoming carriers to the Golgi membranes (Duran et al., 2012). SM has been proposed to form lipid domains together with cholesterol in cellular membranes (Simons and van Meer, 1988; Kusumi et al., 2004; Goswami et al., 2008; Brameshuber et al., 2010; Maxfield and van Meer, 2010; Simons and Gerl, 2010; Sezgin and Schwille, 2011; Simons and Sampaio, 2011; Surma et al., 2011). One reasonable hypothesis is that SM levels, by regulating the lateral order of the Golgi membranes (Gkantiragas et al., 2001; Klemm et al., 2009; Bankaitis et al., 2012), control transport carrier formation by recruiting various proteins at a specific budding site. To test this hypothesis, we asked whether a relatively simpler reaction by which a Golgi-specific glycosylation enzyme glycosylates its substrates is dependent on SM homeostasis. We now show that disruption of SM homeostasis by using short-chain ceramide affects the organization of the TGN in such a way that the enzyme sialyltransferase (ST) fails to interact with its substrate and thus creates a glycosylation defect.

Results and discussion

SM is generated by the SM synthase (SMS) enzymes, which convert ceramide and phosphatidylcholine to SM and diacylglycerol, respectively. SMS1 localizes to the trans-Golgi membranes,

J. van Galen and F. Campelo contributed equally to this paper.

Correspondence to Vivek Malhotra: vivek.malhotra@crg.eu.

Abbreviations used in this paper: CARTS, carriers of the TGN to the cell surface; FKBP, FK506-binding protein; FRB, FKBP–rapamycin binding; PAUF, pancreatic adenocarcinoma up-regulated factor; SM, sphingomyelin; SMS, SM synthase; ST, sialyltransferase.

The Rockefeller University Press $30.00
J. Cell Biol. Vol. 206 No. 5 609–618
www.jcb.org/cgi/doi/10.1083/jcb.201405009

whereas SMS2 is found predominantly at the cell surface (Huitema et al., 2004). In addition, an ER-localized, SMS-related protein has been identified, which could also affect SM homeostasis at the Golgi complex (Vacaru et al., 2009). An RNAi-based approach to study the role of SM in Golgi membrane organization is unfavorable, as it requires several days of knockdown and will not lead to depletion of the previously assembled pools of SM in the membranes. To investigate the role SM plays in controlling Golgi membrane functions, we perturb SM homeostasis by treating cells with D-ceramide-C6 (D-cer-C6; Rosenwald and Pagano, 1993; Duran et al., 2012). This treatment does not affect the overall levels of SM but produces a pool of short-chain SM that accounts for >20% of the total SM in the Golgi membranes (Duran et al., 2012). We have therefore used this approach to test the requirement of SM in the organization and function of transmembrane proteins in the Golgi complex.

Treatment with D-cer-C6 alters the organization of Golgi membranes

As reported previously, perturbation of SM levels by treating cells with 20 µM D-cer-C6 blocks transport carrier biogenesis and protein transport at the Golgi complex (Duran et al., 2012). To test whether SM organization also plays a role in the organization of Golgi proteins, HeLa cells expressing the Golgi marker mannosidase II–GFP were treated for 4 h with D-cer-C6, its nonmetabolizable stereoisomer L-ceramide-C6 (L-cer-C6), or carrier as a control, and the localization of mannosidase II–GFP and the Golgi protein GRASP65 (Barr et al., 1998) was investigated by immunofluorescence microscopy. In control and L-cer-C6–treated cells, mannosidase II–GFP and GRASP65 colocalize in the perinuclear area (Fig. 1 A); however, in D-cer-C6–treated cells, these proteins are separated from each other (Fig. 1, A and D). Under the same experimental conditions, we investigated the localization of p230 and TGN46, two proteins of the TGN. In both control and L-cer-C6–treated cells, these two proteins show a high degree of colocalization, whereas in D-cer-C6–treated cells, the distribution of these two proteins is disrupted (Fig. 1, B and D). Similar results were obtained when the localization of the TGN marker ST-GFP and TGN46 was investigated (Fig. 1, C and D). It was previously shown that complex sphingolipid biosynthesis is required for the retention of a Golgi-resident mannosyltransferase in yeast (Wood et al., 2012). Our findings show that the localization of Golgi-specific proteins to the respective cisternae is perturbed upon affecting the levels of SM in mammalian cells.

We tested the effects of D-cer-C6 on the Golgi membrane morphology by visualizing the ultrastructure of the cells by electron microscopy. The Golgi stacks appeared to be composed of curled, concentric cisternae upon treatment with D-cer-C6 compared with the flat cisternae in carrier (ethanol) or L-cer-C6–treated cells (Fig. 2 A). We confirmed that these curled membranes contain the TGN marker ST-GFP by cryoimmunoelectron microscopy (Fig. 2 B).

Metabolism of D-cer-C6 into C6-SM by SMS1 and SMS2 leads to disorganization of Golgi membranes

We reported previously that upon treatment of cells with D-cer-C6, C6-SM is generated by SMS1 and SMS2, which replaces endogenous SM and ultimately leads to inhibition of protein exit from the Golgi complex (Duran et al., 2012). To test whether formation of C6-SM from D-cer-C6 plays a role in the observed effects in Golgi compartmentalization (Fig. 1), SMS1 and SMS2 were knocked down in HeLa cells by siRNA. Measurement of the knockdown efficiency by RT-PCR showed a reduction in SMS1 and SMS2 mRNA levels by 65 and 50%, respectively, compared with control siRNA–transfected cells (Fig. 3 A). HeLa cells transfected with control or SMS1 and SMS2 siRNA were treated with ethanol, 20 µM L-cer-C6, or 20 µM D-cer-C6 for 4 h, and the localization of the two TGN proteins p230 and TGN46 was assessed by immunofluorescence microscopy. In control siRNA–transfected cells, after D-cer-C6 treatment, we observed an altered TGN morphology and segregation of both proteins within the TGN as compared with both ethanol- or L-cer-C6–treated cells (Fig. 3, B [top] and C). However, the change in the location of these proteins with respect to each other upon D-cer-C6 treatment was inhibited in cells in which SMS1 and SMS2 were knocked down (Fig. 3, B [bottom] and C). Collectively, these results indicate that the observed effects on the compartmentalization and morphology of the different Golgi cisternae after D-cer-C6 treatment are caused by the conversion of this lipid to C6-SM. In addition, our previously reported results on the lipid profile of Golgi membranes from cells treated with D-cer-C6 showed that the formation of the C6-SM occurred at the expense of endogenous long-chain SM, whereas the total levels of SM remained constant (Duran et al., 2012). Our results hence show the importance of regulated levels of SM for the lateral organization of Golgi proteins.

Altered SM levels affect protein glycosylation

As the localization of Golgi glycosylation enzymes is affected by treatment with D-cer-C6 (Fig. 1), we investigated whether protein glycosylation was also affected. TGN46 is a transmembrane protein that is localized to the TGN and cycles between the TGN and the plasma membrane (Banting and Ponnambalam, 1997). The core protein of TGN46 has a molecular mass of 46 kD, but as a result of various glycosylations occurring at the ER and the Golgi complex, the mature protein has an apparent molecular mass of ∼110 kD (Prescott et al., 1997). HeLa cells were treated with increasing concentrations of D-cer-C6 for 4 h, after which the apparent size of TGN46 was examined by Western blotting. Whereas in cells treated with ethanol or L-cer-C6, TGN46 mainly appears as a fully processed 110-kD band, a smaller form of ∼80 kD becomes the main form upon treatments with increasing concentrations of D-cer-C6, indicating an incomplete processing of the protein (Fig. 4 A). This 80-kD form of TGN46 corresponds to a newly synthesized pool because this band was not evident in cells

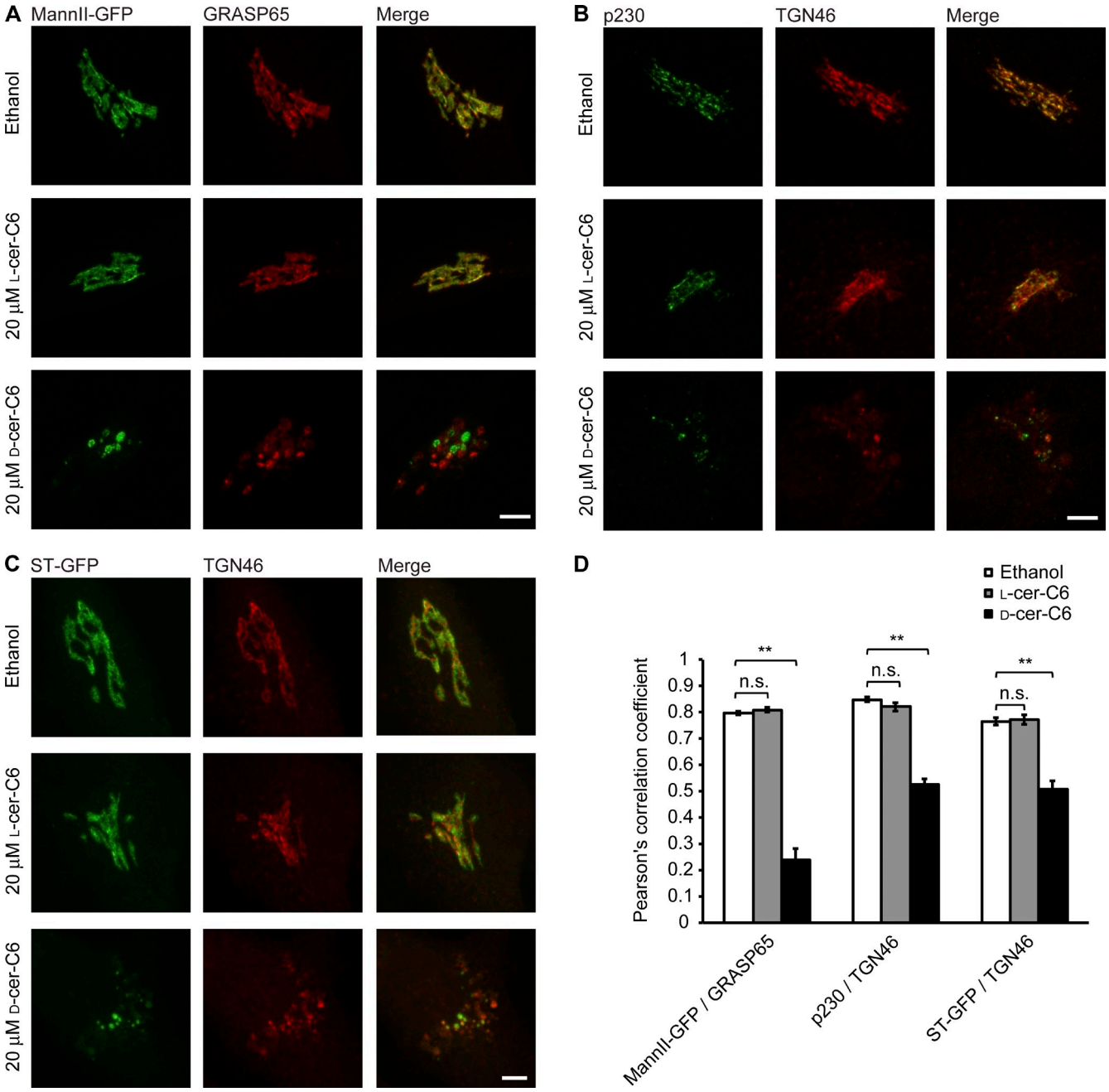

Figure 1. **D-cer-C6 treatment alters Golgi membrane organization.** (A) HeLa cells expressing mannosidase II–GFP (MannII-GFP) were treated with ethanol, 20 µM L-cer-C6, or 20 µM D-cer-C6 for 4 h. The localization of the Golgi markers mannosidase II–GFP and GRASP65 was monitored by immunofluorescence microscopy. (B) HeLa cells were treated with ethanol, 20 µM L-cer-C6, or 20 µM D-cer-C6 for 4 h, and the localization of the TGN markers p230 and TGN46 was monitored by immunofluorescence microscopy. (C) HeLa cells were transfected with sialyltransferase-GFP (ST-GFP) and treated with ethanol, 20 µM L-cer-C6, or 20 µM D-cer-C6 for 4 h. The localization of ST-GFP and TGN46 was monitored by immunofluorescence microscopy. (D) Quantitation of the relative colocalization of the different proteins in the experiments shown in A–C, as measured by the Pearson's correlation coefficient between the green and red channels. Bars show the mean values ± SEM of ≥10 cells counted from three independent experiments. Bars, 5 µm. **, $P < 0.01$.

treated with D-cer-C6 in the presence of cycloheximide to stop new protein synthesis (Fig. S1).

TGN46 is predominantly localized to the TGN, the compartment where glycoproteins are sialylated by the enzyme ST (Stanley, 2011). We tested whether the decrease in molecular mass observed in cells treated with D-cer-C6 was caused by a defect in sialylation of TGN46. Lysates from control and D-cer-C6–treated cells were digested with neuraminidase, an enzyme that removes sialic acid, and TGN46 was analyzed by Western blotting. In control cells, neuraminidase treatment caused a reduction in the apparent molecular mass of TGN46, indicating that fully processed TGN46 is sialylated (Fig. 4 B, left, first and second lanes). However, the 80-kD immature TGN46 present in D-cer-C6–treated cells was not sensitive to neuraminidase digestion (Fig. 4 B, left, third and fourth lanes). These results suggest that treatment with

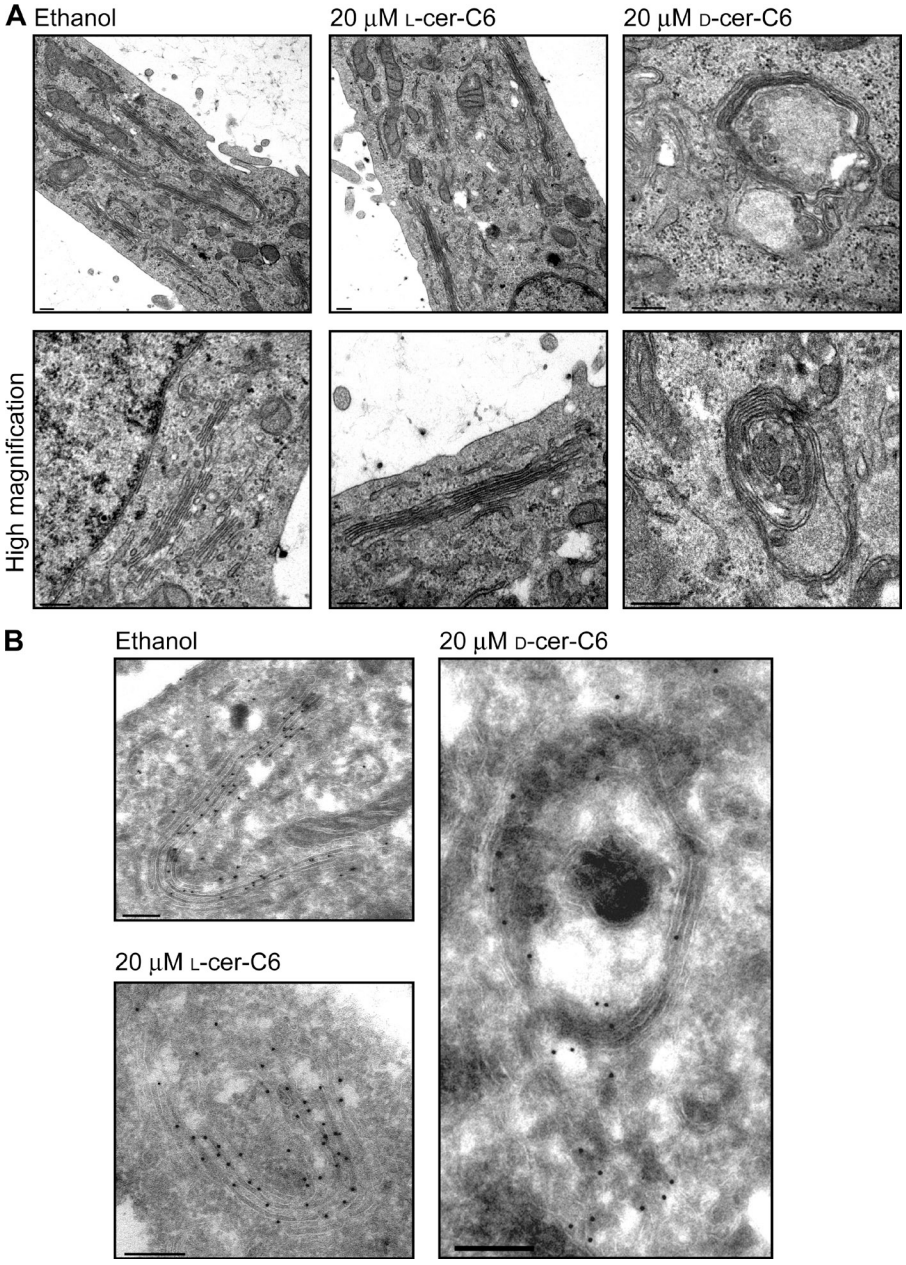

Figure 2. **D-cer-C6 treatment alters Golgi membrane morphology.** (A) HeLa cells were treated with ethanol, 20 μM L-cer-C6, or 20 μM D-cer-C6 for 4 h and fixed, and the morphology of the Golgi membranes was observed by electron microscopy. (B) HeLa cells expressing ST-GFP were treated with ethanol, 20 μM L-cer-C6, or 20 μM D-cer-C6 for 4 h and fixed, and the localization of ST-GFP was visualized by cryo-immunoelectron microscopy. Bars, 200 nm.

D-cer-C6 leads to defects in TGN46 glycosylation, in particular in sialylation. Because D-cer-C6 treatment leads to defects in transport (Duran et al., 2012), a possible explanation for the defect in sialylation is that TGN46 is arrested in the cis-Golgi cisternae before it reaches the trans-Golgi cisternae where it is normally sialylated. To test whether the 80-kD nonsialylated form of TGN46 detected in D-cer-C6–treated cells could be transported through the entire Golgi stack and reach the cell surface, HeLa cells were treated with ethanol or 20 μM D-cer-C6 for 4 h, after which the cells were biotinylated. After precipitation of biotinylated proteins, the size of the cell surface and total TGN46 were examined by Western blotting. Whereas in control cells neuraminidase-sensitive TGN46 appears as a band of 110 kD in the cell surface fractions (Fig. 4 B, right, first and second lanes), in D-cer-C6–treated cells the neuraminidase-insensitive 80-kD band is also detected (Fig. 4 B, right, third and fourth lanes). Presence of the 80-kD band in the cell surface fraction is not caused by cell lysis, as β-actin was not detected in the biotinylated fraction (Fig. 4 B). These results indicate that a small fraction of the smaller form can be transported from the Golgi complex to the cell surface because 20 μM D-cer-C6 treatment does not block its transport completely.

To test whether D-cer-C6 treatment causes a general defect in TGN46 glycosylation, lysates from control or D-cer-C6–treated cells were digested with a commercial mix of different deglycosylation enzymes to remove most N-linked and simple O-linked glycosylations, treated with neuraminidase alone to only remove sialylations, or untreated, and TGN46 was analyzed by Western blotting. In control cells, both deglycosylation treatments showed a reduction in the apparent molecular mass of TGN46, indicating that fully

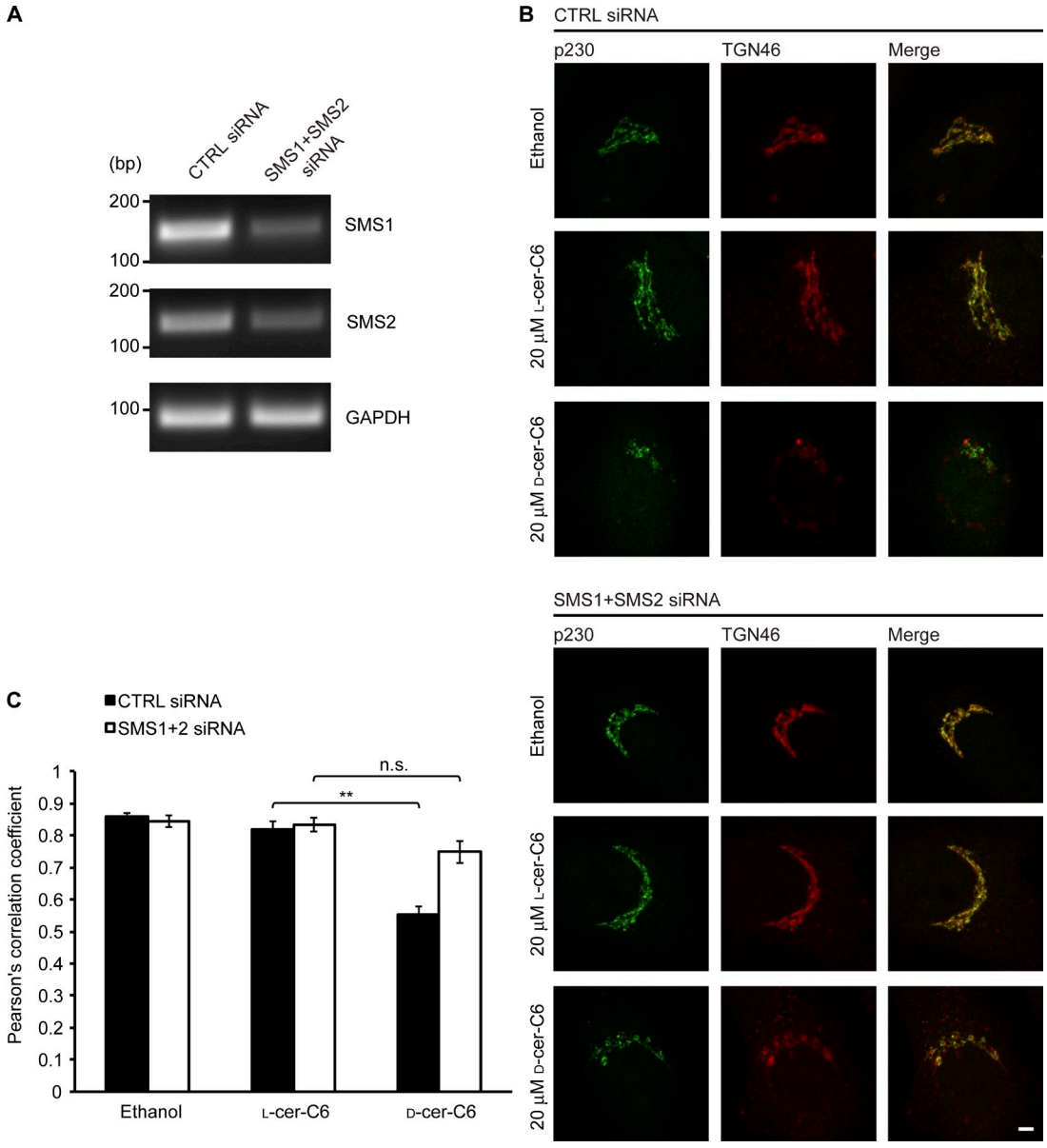

Figure 3. **D-cer-C6–induced Golgi membrane organization defects are mediated by SMS1 and SMS2.** (A) HeLa cells were transfected with control (CTRL) siRNA or with SMS1 and SMS2 siRNA for 96 h. Total RNA was extracted, and the knockdown efficiency was monitored by RT-PCR using primers for SMS1, SMS2, or GAPDH and loading the products on an agarose gel. (B) HeLa cells grown on coverslips were transfected with control or SMS1 and SMS2 siRNA for 92 h. Then, the cells were treated with ethanol, 20 µM L-cer-C6, or 20 µM D-cer-C6 for 4 h. The cells were then fixed, and the localization of the TGN markers p230 and TGN46 was monitored by immunofluorescence microscopy. Bar, 5 µm. (C) Quantitation of the relative colocalization of p230 and TGN46 in the experiments shown in B, as measured by the Pearson's correlation coefficient between the green and red channels. Bars show the mean values ± SEM of ≥10 cells counted from three independent experiments. **, $P < 0.01$.

processed TGN46 is not only sialylated but contains other glycosylations (Fig. 4 C, first through third lanes). However, although the 80-kD immature TGN46 present in D-cer-C6–treated cells was insensitive to neuraminidase digestion, it was sensitive to the deglycosylation mix (Fig. 4 C, fourth through sixth lanes). These results show that D-cer-C6 treatment does not cause a complete glycosylation defect of TGN46.

To test whether formation of C6-SM from D-cer-C6 is responsible for the observed defects in protein sialylation at the TGN, we treated both control and SMS1 + SMS2 double knockdown cells with ethanol, 20 µM L-cer-C6, or 20 µM D-cer-C6 for 4 h, after which cells were lysed, and the lysates were Western blotted against TGN46 to investigate its glycosylation state and β-actin as a loading control (Fig. 4 D). In control-transfected cells that were treated with ethanol or L-cer-C6, the fully processed 110-kD band was the prominent form of TGN46, ∼70% of the total TGN46, whereas in cells that were treated with D-cer-C6, <40% of the total pool of TGN46 was fully glycosylated (Fig. 4, D and E). However, in SMS1 + SMS2 knockdown cells, the D-cer-C6–mediated block in glycosylation was alleviated, as in these cells ∼60% of TGN46 was fully glycosylated after D-cer-C6 treatment (Fig. 4, D and E). This indicates that conversion of D-cer-C6 to C6-SM leads to a defect in glycosylation.

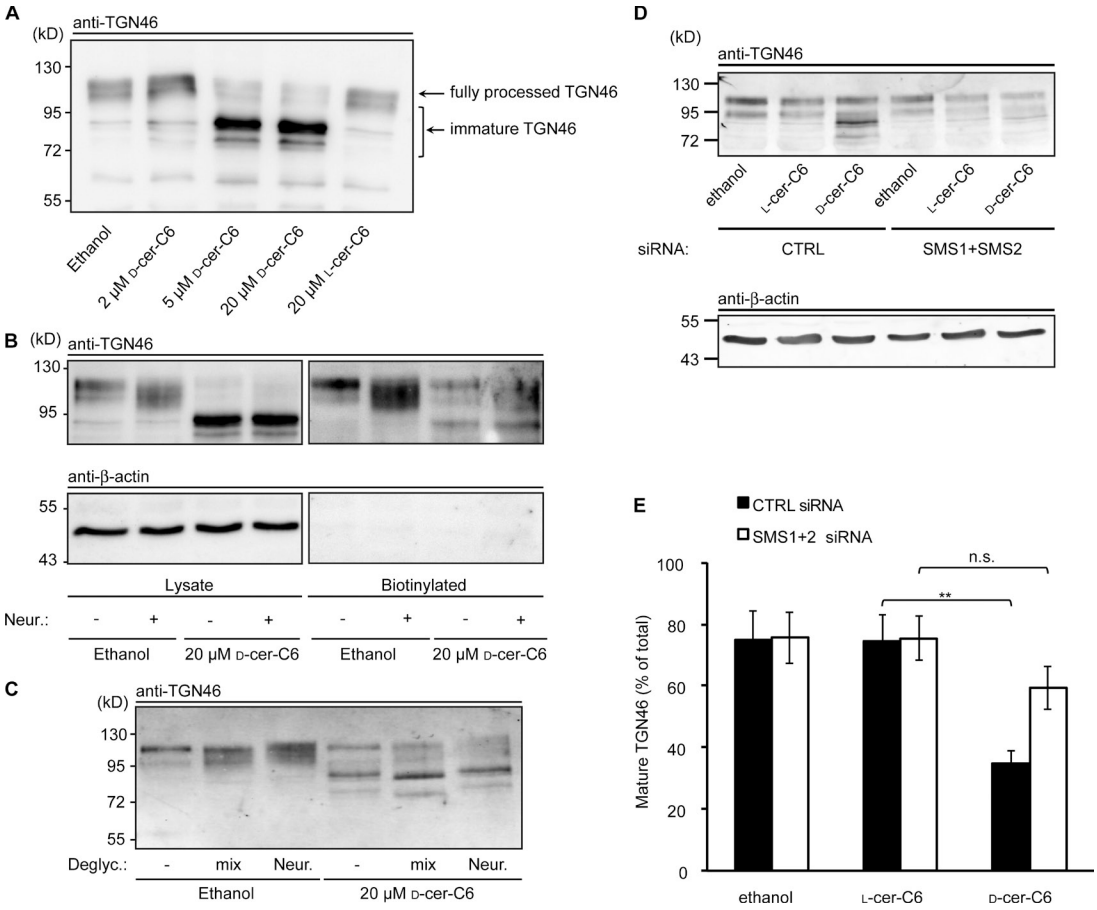

Figure 4. **D-cer-C6 treatment affects TGN46 glycosylation.** (A) HeLa cells were treated with ethanol, the indicated concentrations of D-cer-C6, or 20 µM L-cer-C6 for 4 h, after which the cells were lysed, and the lysates were analyzed by Western blotting using an anti-TGN46 antibody. A 110-kD band corresponds to the fully processed, fully glycosylated TGN46, whereas smaller bands of ∼95, 80, and 75 kD correspond to immature forms of TGN46. (B) HeLa cells were treated with ethanol or 20 µM D-cer-C6 for 4 h, after which the cells were biotinylated. After isolation of biotinylated proteins, the biotinylated fractions and cell lysates were treated with neuraminidase (Neur.) or buffer alone and analyzed by Western blotting using antibodies against TGN46 and β-actin. (C) HeLa cells were treated with ethanol or with 20 µM D-cer-C6 for 4 h, after which the cells were lysed. Lysates were treated with a deglycosylation (Deglyc.) mix (second and fifth lanes), treated with neuraminidase (third and sixth lanes), or remained untreated (first and fourth lanes) and analyzed by Western blotting using an anti-TGN46 antibody. (D) HeLa cells transfected with control (CTRL) or SMS1 + SMS2 siRNA for 92 h were treated with ethanol, 20 µM L-cer-C6, or 20 µM D-cer-C6 for 4 h, after which cells were lysed, and the lysates were analyzed by Western blotting using anti-TGN46 and anti–β-actin antibodies. (E) Quantitation of the band intensity of mature 110-kD TGN46 (in percentages of total TGN46) for the experiment in D. Bars show the mean values ± SEM of four independent experiments (n = 4). Statistical significance is indicated as **, $P < 0.01$ or n.s., $P > 0.05$.

Altered SM levels cause a physical separation of glycosylation enzymes from their substrates

Our results thus far show that treatment of HeLa cells with D-cer-C6 and its conversion to C6-SM caused in TGN46 a sialylation defect, a late glycosylation step occurring at the trans-Golgi complex and the TGN. However, a fraction of this immature TGN46 was transported to the cell surface (Fig. 4). Interestingly, a GFP chimera of ST (ST-GFP), an enzyme responsible for protein sialylation, was physically separated from TGN46 after D-cer-C6 treatment (Fig. 1 C). These results raise the question whether the observed glycosylation defects are caused by a physical segregation of the glycosylating enzymes from their substrates. To test whether TGN46 and ST can be mutually accessible in D-cer-C6–treated cells, we used a rapamycin-mediated trapping assay (Pecot and Malhotra, 2004). Upon binding of the small molecule rapamycin to the FK506-binding protein (FKBP; Wiederrecht et al., 1991), the FKBP–rapamycin complex gains a high affinity for the FKBP–rapamycin-binding (FRB) domain of the FKBP–rapamycin-associated protein (Brown et al., 1994; Sabatini et al., 1994). We generated a construct by inserting an FRB domain in the lumenal side of C-terminally GFP-tagged TGN46 (TGN46-FRB-GFP) and the parallel construct by inserting FKBP in the lumenal side of the Golgi localization domain of ST with a C-terminal RFP tag (ST-FKBP-RFP; Fig. 5 A). When expressed in HeLa cells, both constructs localize to the trans-Golgi cisternae/TGN as observed by fluorescence microscopy, confirming that the added domains do not apparently alter the localization of these proteins (Fig. S2 A). Moreover, TGN46-FRB-GFP localization overlaps with endogenous TGN46 (Fig. S2 B). In addition, TGN46-FRB-GFP localized to numerous punctae, which are in fact transport carriers of the TGN to the cell surface (CARTS) because they colocalize with the CARTS-specific cargo mRFP–pancreatic adenocarcinoma up-regulated factor (PAUF; Fig. S2 C; Wakana et al., 2012) but not with

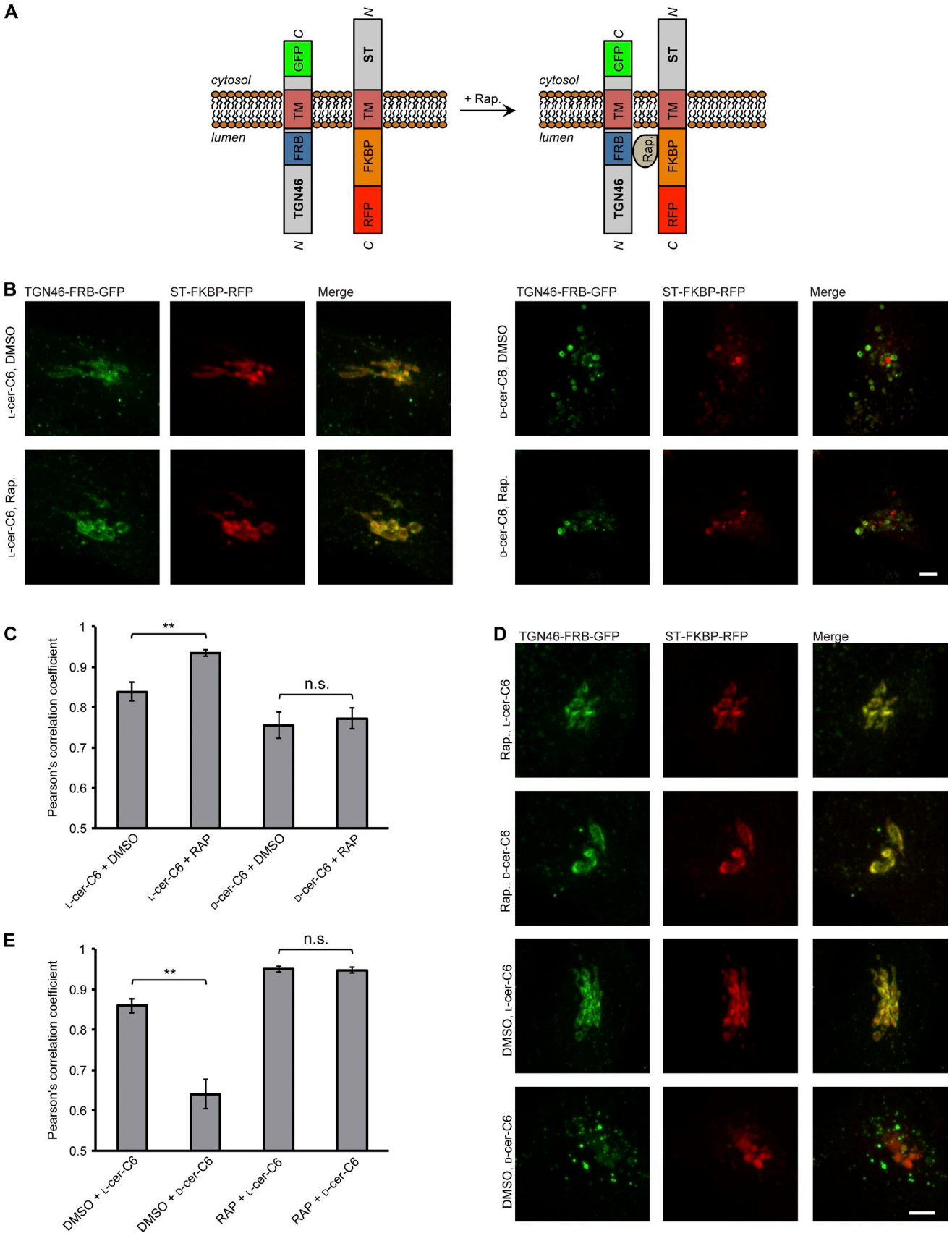

Figure 5. **D-cer-C6 treatment causes permanent segregation of a Golgi-resident enzyme from its substrate.** (A) Scheme of the trapping procedure using rapamycin (Rap.)-mediated dimerization of FRB and FKBP domains. The domain structure of the chimeric constructs TGN46-FRB-GFP and ST-FKBP-RFP is shown relative to the Golgi membrane. Transmembrane (TM), FRB, and FKBP domains and the N and C termini of the proteins are indicated. (B) HeLa cells

proteins specific for the ER exit sites, endosomes, or lysosomes (Fig. S2, D–H). HeLa cells expressing TGN46-FRB-GFP and ST-FKBP-RFP were treated with 20 µM L-cer-C6 or 20 µM D-cer-C6 for 4 h, after which 500 nM rapamycin or DMSO was added and incubation was continued for 2 h in presence of 100 µM cycloheximide to block protein synthesis. In L-cer-C6–treated cells, treatment with rapamycin increased the level of colocalization of the two proteins compared with DMSO-treated cells, as measured by the Pearson's correlation coefficient between the two channels (Fig. 5, B and C). However, in D-cer-C6–treated cells, rapamycin treatment did not induce a coalescence of the two proteins in the same domains and the Pearson's correlation coefficient remained unaltered compared with DMSO-treated cells (Fig. 5, B and C). To corroborate that treatment with D-cer-C6 by itself does not alter the trapping capacity of rapamycin, HeLa cells expressing TGN46-FRB-GFP and ST-FKBP-RFP were incubated with 500 nM rapamycin or DMSO for 2 h, after which the incubation was continued for 4 h in the presence of 20 µM L-cer-C6 or 20 µM D-cer-C6 and 100 µM cycloheximide, before fixation for fluorescence microscopy. Pretreatment with rapamycin, but not with DMSO, inhibited the lateral segregation of TGN46-FRB-GFP from ST-FKBP-RFP because these two proteins were present in the same membrane compartments (Fig. 5, D and E). Altogether, these results indicate that TGN46-FRB-GFP and ST-FKBP-RFP are not mutually accessible after D-cer-C6 treatment, suggesting that a physical separation is the cause for the observed sialylation defect in endogenous TGN46.

In summary, our results show that conversion of short-chain ceramide into short-chain SM mediated by SMS segregates Golgi proteins. Specifically, this leads to a physical separation of the enzyme ST from its substrate TGN46 that, as a result, is not sialylated. It is possible that under these conditions, newly synthesized TGN46 arrives in the Golgi complex, is modified by the enzymes of the early Golgi cisternae, and exits the Golgi complex for the cell surface without entering the TGN (Patterson et al., 2008). However, we prefer to propose that SM homeostasis is important for the lipid organization into membrane domains of different thickness commensurate with the length of the protein transmembrane domains (Munro, 1995). When this homeostasis is perturbed with short-chain ceramide treatment, lipid mixing occurs, and the lipid bilayer becomes laterally homogeneous. Because of the resulting changes in lipid bilayer thickness, the membrane cannot optimally accommodate proteins with long transmembrane domains. This, we propose, leads to a physical separation of the enzymes (ST) and the substrates (TGN46) in different domains within the same Golgi cisternae. These findings highlight the significance of lipid homeostasis in protein organization and function at the TGN.

Materials and methods

Reagents and antibodies

N-hexanoyl-D-erythro-sphingosine (D-cer-C6) and *N*-hexanoyl-L-erythro-sphingosine (L-cer-C6) obtained from Matreya were dissolved in pure ethanol (Merck) as stock solution. Cycloheximide was purchased from A.G. Scientific, rapamycin was obtained from EMD Millipore, and both were dissolved in DMSO as stock solutions. Sheep anti–human TGN46 was obtained from AbD Serotec. Goat anti-GRASP65 (C-20) was obtained from Santa Cruz Biotechnology, Inc. Mouse anti–β-actin (clone AC-15) was obtained from Sigma-Aldrich. Rabbit polyclonal antibody against GFP was purchased from Abcam. Mouse anti-p230, mouse anti-Sec31a, and mouse anti-EEA1 were obtained from BD. Mouse anti-M6PR (mannose-6 phosphate receptor) was obtained from Thermo Fisher Scientific, mouse anti–transferrin receptor was purchased from Invitrogen, and mouse anti-LAMP1 was obtained from Stressgen. Alexa Fluor–labeled secondary antibodies were obtained from Invitrogen, and HRP-conjugated secondary antibodies were purchased from Santa Cruz Biotechnology, Inc. Protein A–gold was obtained from the Department of Cell Biology at Utrecht University (Utrecht, Netherlands).

Cell culture, RNAi, and plasmids

HeLa cells were cultured in DMEM (Lonza) containing 10% FCS. Cells were transfected using X-tremeGENE 9 (Roche) or TransIT-HeLaMONSTER (Mirus Bio LLC) following the manufacturer's recommendations. siRNA transfection was performed using HiPerFect transfection reagent (QIAGEN) following the manufacturer's protocol. The nontargeting control siRNA oligonucleotide sequence was 5′-AAUUGCGUAGUCUAAGUUAAAGUGG-3′ (Invitrogen); siRNA oligonucleotides against SMS1 and SMS2 were Silencer Select Predesigned siRNA obtained from Ambion with IDs s48915 and s46644 (catalog no. 4392420), respectively (Duran et al., 2012). ST-GFP, encoding for the ST6Gal-I ST, and ST-FKBP-RFP plasmids were cloned from the previously described ST-FKBP-GFP plasmid (Pecot and Malhotra, 2004) into pEGFP-N1 and pcDNA3.1-mCherry vectors, respectively. HeLa cells stably expressing the plasmid encoding the first 100 amino acids of rat mannosidase II in the pEGFP-N1 vector were described previously (Sütterlin et al., 2005). The TGN46-GFP plasmid, generated by inserting human TGN46 cDNA into a pEGFP-N1 vector using the BamHI restriction site, was provided by S. Ponnambalam (Leeds University, Leeds, England, UK) and used to clone the plasmid encoding TGN46-FRB-GFP, by inserting the FRB domain from pFA6a-FRB-GFP-kanMX6, described in Haruki et al. (2008) and obtained from EUROSCARF (European Saccharomyces Cerevisiae Archive for Functional Analysis), by Gibson assembly (Gibson et al., 2009) with two PCRs using the following primers: 5′-AGCGCGGAGAGCAGC-3′ and 3′-GCCATTTCCAGAACCGTTCGG-5′ to amplify TGN46-GFP and 5′-CGGTTCTGGAAATGGCATCCTCTGGCATGAGATGTGGCATG-3′ and 3′-GCTGCTCTCCGCGCTCTTTGAGATTCGTCGGAACACATGATAATAGAG-5′ to amplify the FRB domain from the pFA6a-FRB-GFP-kanMX6 vector. The mRFP-PAUF plasmid was previously described as a pcDNA3-based vector encoding mRFP to express PAUF with C-terminal mRFP (Wakana et al., 2012). SnapGene software (obtained from GSL Biotech) was used for molecular cloning procedures.

RT-PCR

96 h after siRNA transfection, total RNA was extracted using the RNeasy Mini kit obtained from QIAGEN. The levels of SMS1, SMS2, and GAPDH mRNA were analyzed using Cloned AMV First-Strand cDNA Synthesis kit (Invitrogen) and JumpStart *Taq* DNA Polymerase (Sigma-Aldrich) following the manufacturer's recommendations, using 250 ng of total RNA per reaction. Primers used for PCR are the following: SMS1, 5′-ACTGTGAGCCTCTGGAGCAT-3′ and

expressing TGN46-FRB-GFP and ST-FKBP-RFP were treated with 20 µM L-cer-C6 or 20 µM D-cer-C6 for 4 h, after which 100 µM cycloheximide and DMSO or 500 nM rapamycin was added to the culture media for an additional 2 h. Cells were then fixed for fluorescence microscopy. (C) Quantitation of the relative colocalization of TGN46-FRB-GFP and ST-FKBP-RFP in the experiment shown in B, as measured by the Pearson's correlation coefficient between the green and red channels. Bars show the mean values ± SEM of ≥10 cells counted from four independent experiments. (D) HeLa cells expressing TGN46-FRB-GFP and ST-FKBP-RFP were treated with DMSO or 500 nM rapamycin for 2 h, after which 100 µM cycloheximide and 20 µM L-cer-C6 or 20 µM D-cer-C6 were added to the culture media for an additional 4 h. Cells were then fixed, and the localization of TGN46-FRB-GFP and ST-FKBP-RFP was monitored by fluorescence microscopy. (E) Quantitation of the relative colocalization of TGN46-FRB-GFP and ST-FKBP-RFP in the experiment shown in D, as measured by the Pearson's correlation coefficient between the green and red channels. Bars show the mean values ± SEM of ≥10 cells counted from four independent experiments. **, $P < 0.01$. Bars, 5 µm.

5′-TGCTCCATTTTCAGGGTTTC-3′; SMS2, 5′-CAATTCCTTGCTGCTTCTCC-3′ and 5′-CCTTTGTTTTGCTCCTCAG-3′; and GAPDH, 5′-TGCACCACCAACTGCTTAGC-3′ and 5′-GGCATGGACTGTGGTCATGAG-3′.

Immunofluorescence microscopy

Samples were fixed with 4% formaldehyde in PBS for 20 min, permeabilized with 0.2% Triton X-100 in PBS for 30 min, and blocked in 2% BSA in PBS for 30 min before antibody staining. For Sec31a immunostaining, samples were fixed in methanol for 6 min at −20°C and blocked in 2% BSA in PBS for 30 min at room temperature before antibody staining. Fixed samples were analyzed with a confocal system (TCS SP5 II CW STED; Leica) in confocal mode using a 100×, 1.4 NA objective and detectors (HyD; Leica). Alexa Fluor 488–, 555-, 594-, and 647-conjugated secondary antibodies were used. Images were acquired using the Leica software and converted to TIFF files using ImageJ (version 1.43; National Institutes of Health). Two-channel colocalization analysis was performed using ImageJ, and the Pearson's correlation coefficient was calculated using the Manders' coefficients plugin developed at the Wright Cell Imaging Facility (Toronto, Ontario, Canada).

Electron microscopy

For conventional electron microscopy, HeLa cells treated with ethanol, L-cer-C6, or D-cer-C6 were fixed for 2 h with 2% glutaraldehyde buffered with 0.2 M sodium cacodylate containing 0.05% $CaCl_2$, pH 7.4. The samples were postfixed for 2 h in a 1:1 mixture of 2% aqueous osmium tetroxide and 3% aqueous potassium ferrocyanide. The samples were dehydrated in ethanol and embedded in Epon. Sections were mounted on copper grids and counterstained with uranyl acetate and lead citrate.

For cryoimmunoelectron microscopy, samples were fixed with 2% paraformaldehyde and 0.2% glutaraldehyde in 0.1 M sodium phosphate buffer, pH 7.4. After washing in buffer, the cells were pelleted by centrifugation, embedded in 10% gelatin, cooled on ice, and cut into 1-mm^3 blocks. The blocks were infused with 2.3 M sucrose at 4°C overnight, frozen in liquid nitrogen, and stored until cryo-ultramicrotomy. Sections (~50 nm thick) were cut at −120°C with a diamond knife in an ultramicrotome (Ultracut T/FCS; Leica). Ultrathin sections were picked up in a mix of 1.8% methylcellulose and 2.3 M sucrose (1:1). Cryosections were collected on carbon- and formvar-coated copper grids and incubated with rabbit polyclonal antibodies against GFP followed by protein A–gold. After labeling, the sections were treated with 1% glutaraldehyde, counterstained with uranyl acetate, pH 7.0, and embedded in methyl cellulose-uranyl acetate, pH 4.0 (9:1). Grids were examined with an electron microscope (JEM-1011; Jeol).

Cell surface biotinylation

HeLa cells were treated with ethanol or 20 µM D-cer-C6 for 4 h at 37°C, after which the cells were washed three times with ice-cold PBS+ (PBS with 0.1 mM $CaCl_2$ and 0.1 mM $MgCl_2$). The cells were biotinylated with 1 mg/ml sulfo-NHS-LC-Biotin (Thermo Fisher Scientific) in PBS+ for 30 min on ice. The cells were washed twice with PBS+, and biotin was quenched by incubation with 100 mM glycine in PBS+ for 30 min on ice. After washing twice with PBS+, the cells were lysed with PBS containing 2% NP-40, 0.2% SDS, and protease inhibitors for 10 min on ice. The lysates were centrifuged for 15 min at 16,000 *g*, and the resulting supernatants were incubated with equilibrated NeutrAvidin agarose resin (Thermo Fisher Scientific) overnight at 4°C while rotating. The resins were washed four times with PBS containing 2% NP-40 and 0.2% SDS and twice with PBS. The resin was eluted by incubation in denaturing buffer (New England Biolabs, Inc.) for 5 min at 95°C.

Protein deglycosylation

Protein digestion with neuraminidase (New England Biolabs, Inc.) or with a Protein Deglycosylation Mix (New England Biolabs, Inc.) containing neuraminidase, PNGase F, *O*-glycosidase, β(1–4) galactosidase, and β-*N*-acetylglucosaminidase was performed according to the manufacturer's guidelines.

Statistics

Statistical significance was tested using Student's *t* test. Different datasets were considered to be statistically significant when $P < 0.05$ or $P < 0.01$.

Online supplemental material

Fig. S1 shows that the 80-kD form of TGN46 observed in D-cer-C6–treated cells is newly synthesized. Fig. S2 shows the localization of TGN46-FRB-GFP and ST-FKBP-RFP with a TGN marker and that of TGN46-FRB-GFP with different intracellular membranes. Online supplemental material is available at http://www.jcb.org/cgi/content/full/jcb.201405009/DC1.

We thank the members of the Malhotra laboratory for valuable discussions. We thank Dr. S. Ponnambalam for the kind gift of the TGN46-GFP construct. We thank Dr. K. Saito for cloning ST-FKBP-RFP. All confocal imaging was performed in the Center for Genomic Regulation Advanced Light Microscopy Unit.

We acknowledge support from the Spanish Ministry of Economy and Competitiveness, "Centro de Excelencia Severo Ochoa 2013–2017" (SEV-2012-0208). F. Campelo was partially funded by a Juan de la Cierva fellowship. V. Malhotra is an Institució Catalana de Recerca i Estudis Avançats professor at the Center for Genomic Regulation, and the work in his laboratory is funded by grants from Plan Nacional (BFU2008-00414), Consolider (CSD2009-00016), Agència de Gestió d'Ajuts Universitaris i de Recerca (AGAUR) Grups de Recerca Emergents (SGR2009-1488; AGAUR-Catalan Government), and the European Research Council (268692). The project has received research funding from the European Union. This paper reflects only the author's views. The Union is not liable for any use that may be made of the information contained therein.

The authors declare no competing financial interests.

Submitted: 2 May 2014
Accepted: 30 July 2014

References

Bankaitis, V.A., R. Garcia-Mata, and C.J. Mousley. 2012. Golgi membrane dynamics and lipid metabolism. *Curr. Biol.* 22:R414–R424. http://dx.doi.org/10.1016/j.cub.2012.03.004

Banting, G., and S. Ponnambalam. 1997. TGN38 and its orthologues: roles in post-TGN vesicle formation and maintenance of TGN morphology. *Biochim. Biophys. Acta.* 1355:209–217. http://dx.doi.org/10.1016/S0167-4889(96)00146-2

Barr, F.A., N. Nakamura, and G. Warren. 1998. Mapping the interaction between GRASP65 and GM130, components of a protein complex involved in the stacking of Golgi cisternae. *EMBO J.* 17:3258–3268. http://dx.doi.org/10.1093/emboj/17.12.3258

Brameshuber, M., J. Weghuber, V. Ruprecht, I. Gombos, I. Horváth, L. Vigh, P. Eckerstorfer, E. Kiss, H. Stockinger, and G.J. Schütz. 2010. Imaging of mobile long-lived nanoplatforms in the live cell plasma membrane. *J. Biol. Chem.* 285:41765–41771. http://dx.doi.org/10.1074/jbc.M110.182121

Brown, E.J., M.W. Albers, T.B. Shin, K. Ichikawa, C.T. Keith, W.S. Lane, and S.L. Schreiber. 1994. A mammalian protein targeted by G1-arresting rapamycin-receptor complex. *Nature*. 369:756–758. http://dx.doi.org/10.1038/369756a0

Duran, J.M., F. Campelo, J. van Galen, T. Sachsenheimer, J. Sot, M.V. Egorov, C. Rentero, C. Enrich, R.S. Polishchuk, F.M. Goñi, et al. 2012. Sphingomyelin organization is required for vesicle biogenesis at the Golgi complex. *EMBO J.* 31:4535–4546. http://dx.doi.org/10.1038/emboj.2012.317

Gibson, D.G., L. Young, R.Y. Chuang, J.C. Venter, C.A. Hutchison III, and H.O. Smith. 2009. Enzymatic assembly of DNA molecules up to several hundred kilobases. *Nat. Methods*. 6:343–345. http://dx.doi.org/10.1038/nmeth.1318

Gkantiragas, I., B. Brügger, E. Stüven, D. Kaloyanova, X.Y. Li, K. Löhr, F. Lottspeich, F.T. Wieland, and J.B. Helms. 2001. Sphingomyelin-enriched microdomains at the Golgi complex. *Mol. Biol. Cell*. 12:1819–1833. http://dx.doi.org/10.1091/mbc.12.6.1819

Goswami, D., K. Gowrishankar, S. Bilgrami, S. Ghosh, R. Raghupathy, R. Chadda, R. Vishwakarma, M. Rao, and S. Mayor. 2008. Nanoclusters of GPI-anchored proteins are formed by cortical actin-driven activity. *Cell*. 135:1085–1097. http://dx.doi.org/10.1016/j.cell.2008.11.032

Haruki, H., J. Nishikawa, and U.K. Laemmli. 2008. The anchor-away technique: rapid, conditional establishment of yeast mutant phenotypes. *Mol. Cell*. 31:925–932. http://dx.doi.org/10.1016/j.molcel.2008.07.020

Huitema, K., J. van den Dikkenberg, J.F. Brouwers, and J.C. Holthuis. 2004. Identification of a family of animal sphingomyelin synthases. *EMBO J.* 23:33–44. http://dx.doi.org/10.1038/sj.emboj.7600034

Klemm, R.W., C.S. Ejsing, M.A. Surma, H.J. Kaiser, M.J. Gerl, J.L. Sampaio, Q. de Robillard, C. Ferguson, T.J. Proszynski, A. Shevchenko, and K. Simons. 2009. Segregation of sphingolipids and sterols during formation of secretory vesicles at the trans-Golgi network. *J. Cell Biol.* 185:601–612. http://dx.doi.org/10.1083/jcb.200901145

Kusumi, A., I. Koyama-Honda, and K. Suzuki. 2004. Molecular dynamics and interactions for creation of stimulation-induced stabilized rafts from small unstable steady-state rafts. *Traffic*. 5:213–230. http://dx.doi.org/10.1111/j.1600-0854.2004.0178.x

Maxfield, F.R., and G. van Meer. 2010. Cholesterol, the central lipid of mammalian cells. *Curr. Opin. Cell Biol.* 22:422–429. http://dx.doi.org/10.1016/j.ceb.2010.05.004

Munro, S. 1995. An investigation of the role of transmembrane domains in Golgi protein retention. *EMBO J.* 14:4695–4704.

Patterson, G.H., K. Hirschberg, R.S. Polishchuk, D. Gerlich, R.D. Phair, and J. Lippincott-Schwartz. 2008. Transport through the Golgi apparatus by rapid partitioning within a two-phase membrane system. *Cell*. 133:1055–1067. http://dx.doi.org/10.1016/j.cell.2008.04.044

Pecot, M.Y., and V. Malhotra. 2004. Golgi membranes remain segregated from the endoplasmic reticulum during mitosis in mammalian cells. *Cell*. 116:99–107. http://dx.doi.org/10.1016/S0092-8674(03)01068-7

Prescott, A.R., J.M. Lucocq, J. James, J.M. Lister, and S. Ponnambalam. 1997. Distinct compartmentalization of TGN46 and beta 1,4-galactosyltransferase in HeLa cells. *Eur. J. Cell Biol.* 72:238–246.

Rosenwald, A.G., and R.E. Pagano. 1993. Inhibition of glycoprotein traffic through the secretory pathway by ceramide. *J. Biol. Chem.* 268:4577–4579.

Sabatini, D.M., H. Erdjument-Bromage, M. Lui, P. Tempst, and S.H. Snyder. 1994. RAFT1: a mammalian protein that binds to FKBP12 in a rapamycin-dependent fashion and is homologous to yeast TORs. *Cell*. 78:35–43. http://dx.doi.org/10.1016/0092-8674(94)90570-3

Sezgin, E., and P. Schwille. 2011. Fluorescence techniques to study lipid dynamics. *Cold Spring Harb. Perspect. Biol.* 3:a009803. http://dx.doi.org/10.1101/cshperspect.a009803

Simons, K., and M.J. Gerl. 2010. Revitalizing membrane rafts: new tools and insights. *Nat. Rev. Mol. Cell Biol.* 11:688–699. http://dx.doi.org/10.1038/nrm2977

Simons, K., and J.L. Sampaio. 2011. Membrane organization and lipid rafts. *Cold Spring Harb. Perspect. Biol.* 3:a004697. http://dx.doi.org/10.1101/cshperspect.a004697

Simons, K., and G. van Meer. 1988. Lipid sorting in epithelial cells. *Biochemistry*. 27:6197–6202. http://dx.doi.org/10.1021/bi00417a001

Stanley, P. 2011. Golgi glycosylation. *Cold Spring Harb. Perspect. Biol.* 3:a005199. http://dx.doi.org/10.1101/cshperspect.a005199

Surma, M.A., C. Klose, R.W. Klemm, C.S. Ejsing, and K. Simons. 2011. Generic sorting of raft lipids into secretory vesicles in yeast. *Traffic*. 12:1139–1147. http://dx.doi.org/10.1111/j.1600-0854.2011.01221.x

Sütterlin, C., R. Polishchuk, M. Pecot, and V. Malhotra. 2005. The Golgi-associated protein GRASP65 regulates spindle dynamics and is essential for cell division. *Mol. Biol. Cell*. 16:3211–3222. http://dx.doi.org/10.1091/mbc.E04-12-1065

Vacaru, A.M., F.G. Tafesse, P. Ternes, V. Kondylis, M. Hermansson, J.F. Brouwers, P. Somerharju, C. Rabouille, and J.C. Holthuis. 2009. Sphingomyelin synthase-related protein SMSr controls ceramide homeostasis in the ER. *J. Cell Biol.* 185:1013–1027. http://dx.doi.org/10.1083/jcb.200903152

Wakana, Y., J. van Galen, F. Meissner, M. Scarpa, R.S. Polishchuk, M. Mann, and V. Malhotra. 2012. A new class of carriers that transport selective cargo from the trans Golgi network to the cell surface. *EMBO J.* 31:3976–3990. http://dx.doi.org/10.1038/emboj.2012.235

Wiederrecht, G., L. Brizuela, K. Elliston, N.H. Sigal, and J.J. Siekierka. 1991. FKB1 encodes a nonessential FK 506-binding protein in *Saccharomyces cerevisiae* and contains regions suggesting homology to the cyclophilins. *Proc. Natl. Acad. Sci. USA*. 88:1029–1033. http://dx.doi.org/10.1073/pnas.88.3.1029

Wood, C.S., C.S. Hung, Y.S. Huoh, C.J. Mousley, C.J. Stefan, V. Bankaitis, K.M. Ferguson, and C.G. Burd. 2012. Local control of phosphatidylinositol 4-phosphate signaling in the Golgi apparatus by Vps74 and Sac1 phosphoinositide phosphatase. *Mol. Biol. Cell*. 23:2527–2536. http://dx.doi.org/10.1091/mbc.E12-01-0077